

# A comparative study of oxygen storage capacity over $\text{Ce}_{0.6}\text{Zr}_{0.4}\text{O}_2$ mixed oxides investigated by temperature-programmed reduction and dynamic OSC measurements

N. Hickey<sup>a</sup>, P. Fornasiero<sup>a</sup>, R. Di Monte<sup>a</sup>, J. Kaspar<sup>a,\*</sup>, M. Graziani<sup>a</sup> and G. Dolcetti<sup>b</sup>

<sup>a</sup> Dipartimento di Scienze Chimiche, via Giorgieri 1, Università di Trieste, 34127 Trieste, Italy

E-mail: kaspar@univ.trieste.it

<sup>b</sup> Dipartimento di Scienze e Tecnologie Chimiche, via Cotonificio 108, Università di Udine, 33100 Udine, Italy

Received 31 August 2000; accepted 18 December 2000

The effects of redox-ageing on the temperature-programmed reduction and dynamic oxygen storage were investigated on two samples of  $\text{Ce}_{0.6}\text{Zr}_{0.4}\text{O}_2$  prepared under different synthesis conditions. It was observed that a high-temperature reduction/mild oxidation redox cycle can generate temperature-programmed reduction (TPR) profiles featuring a reduction peak at a temperature as low as 537 K. However, despite such favourable reduction behaviour, a strong deactivation of the oxygen storage is observed under dynamic conditions, indicating the limitations of the TPR method for investigation of oxygen storage.

**KEY WORDS:** oxygen storage of  $\text{CeO}_2$ – $\text{ZrO}_2$  mixed oxides; three-way catalysts; reduction of  $\text{CeO}_2$ – $\text{ZrO}_2$  solid solutions; dynamic OSC

## 1. Introduction

The redox properties of  $\text{CeO}_2$ – $\text{ZrO}_2$  mixed oxides have received considerable attention in recent years due the extensive use of these materials in advanced three-way catalysts (TWCs) as the so-called oxygen storage material [1]. The oxygen storage/release capacity (OSC) of a three-way catalyst is the ability to attenuate the negative effects of rich/lean oscillations of exhaust gas composition upon pollutant conversion. OSC is usually discussed in terms of the ability to regulate the oxygen partial pressure in the exhaust through the  $\text{Ce}^{3+}/\text{Ce}^{4+}$  redox couple. Of the two processes, oxidation is easy and occurs even at room temperature (rt), while the reduction requires temperatures higher than 473 K [2]. For this reason the reduction rather than oxidation process is usually studied.

Total OSC, which represents the overall amount of transferable oxygen at a fixed temperature, is generally measured by the temperature-programmed reduction (TPR) method [3]. Following the pioneering work of Yao and Yu-Yao [4], dynamic OSC measurement involves alternately pulsing the chosen reducing agent (usually CO but sometimes  $\text{H}_2$ ) and  $\text{O}_2$  over the material under investigation.

Under real exhaust conditions, the air-to-fuel (A/F) ratio oscillates with a frequency of about 1 Hz around the stoichiometric point [5], which in principle makes measurement of redox behaviour under dynamic conditions more relevant than total OSC measurement [3]. However, measurement of dynamic OSC by means of the pulse technique is critically influenced by several factors and no standardised procedure for measuring dynamic OSC has been suggested in

the literature, which makes comparison of the various data reported difficult. In contrast, TPR is a simple technique and it is widely applied for characterisation of reducible materials [6]. In such measurements, the OSC is calculated by calibration of the integrated peak areas of the TPR profile against those of a standard such as CuO. Although this method is not absent from criticism, mainly due to potential contribution of adspecies to TPR profiles [7], nevertheless it is a quick and effective measurement widely employed for characterisation of the OSC property. Generally speaking, a TPR profile featuring a single reduction peak at low temperature is taken as a fingerprint of an effective OSC system [8], even for evaluation of commercial products [9].

The reduction behaviour of  $\text{CeO}_2$ – $\text{ZrO}_2$  and NM/ $\text{CeO}_2$ – $\text{ZrO}_2$  systems shows some peculiar features in that it has been demonstrated that redox-ageing using high-temperature reduction followed by a mild oxidation can effectively promote reduction at low temperatures [10–15]. In contrast, the reduction temperature increases when a high-temperature oxidation is employed instead of the mild treatment [13,16]. In summary, the TPR method is routinely employed to detect the efficiency of the OSC materials; however, evidence exists that the TPR profile may be strongly affected by several factors, including the pre-treatment.

Efforts to produce  $\text{CeO}_2$ – $\text{ZrO}_2$  systems capable of releasing oxygen at low temperatures are on-going. Recently, chemical high-temperature filing using  $\text{AlCl}_3$  was applied to obtain reduction peaks at an exceptionally low temperature in a  $\text{Ce}_{0.45}\text{Zr}_{0.55}\text{O}_2$  mixed oxide [17]. It was claimed that, due to their high efficiency as OSC promoters, such systems would be available for the next generation of automotive exhaust catalysts.

\* To whom correspondence should be addressed.

In this paper two samples of a  $\text{Ce}_{0.6}\text{Zr}_{0.4}\text{O}_2$  mixed oxide featuring remarkably different TPR profiles (low- and high-temperature reduction) were prepared and their TPR behaviour compared with the dynamic OSC behaviour. The aim is to investigate the correlation between the favourable TPR behaviour, i.e., low-temperature reduction; and the dynamic OSC, i.e., rapid alternating of oxidising/reducing condition. The latter technique is considered to be more relevant to real exhaust conditions [3], even though some correlation between dynamic OSC and TPR were reviewed [8]. It is shown that under dynamic OSC conditions, when  $\text{H}_2$  and  $\text{O}_2$  are alternatively pulsed over the catalysts, the redox behaviour is modified *in situ* leading to deactivation of the low-temperature reduction, detected by TPR.

## 2. Experimental

$\text{Ce}_{0.6}\text{Zr}_{0.4}\text{O}_2$  mixed oxides were synthesised as follows: After dissolving appropriate amounts of  $\text{Ce}(\text{NO}_3)_3 \cdot 6\text{H}_2\text{O}$  (41.15%  $\text{CeO}_2$ , Aldrich) and  $\text{ZrO}(\text{NO}_3)_2 \cdot x\text{H}_2\text{O}$  (35.58%  $\text{ZrO}_2$ , Aldrich) in the chosen solvent (see below), citric acid (99.7%, Prolabo) was added in a molar ratio citric acid: M = 2.1 : 1 (M = Ce or Zr). The resulting solution was stirred at rt for at least 12 h before the solvent was eliminated using a rotary evaporator. This firstly yielded a transparent gel, and then, after the evolution of nitrogen oxides, a solid was obtained. This was flash decomposed at 773 K and calcined at this temperature for 5 h to obtain a yellow powder. Hereafter these samples are indicated as CZ-W and CZ-A, when, respectively, water and water-free ethanol was used as solvent. Powder XRD patterns and Raman spectra measured on both fresh and calcined (1273 K, 5 h) samples revealed formation of a  $\text{Ce}_{0.6}\text{Zr}_{0.4}\text{O}_2$  solid solution of  $t''$  symmetry [8]. Lattice parameters of 0.5315 and 0.5317 nm were calculated, respectively, for CZ-W and CZ-A using a Rietveld profile fitting of the powder XRD spectra on samples calcined at 1273 K, 5 h. CZ-A contained about 5 mol% of a  $\text{CeO}_2$ -rich impurity. XRD characterisation of the redox-aged (see below) samples revealed the presence of single phase products with cell parameters of 0.5311 and 0.5306 nm, respectively, for CZ-W and CZ-A.

The cleaning/ageing procedures applied (consecutively) to the samples are summarised in figure 1. In the ageing procedures performed after the *in situ* oxidising cleaning procedure [19] (heating to 823 K for 1 h while pulsing  $\text{O}_2$ , 100  $\mu\text{l}$ ), TPR measurements up to 1273 K (5%  $\text{H}_2$  in Ar, 10  $\text{K min}^{-1}$ , 25  $\text{ml min}^{-1}$ ) served both as a test of the effect of previous pretreatment on the TPR profile and the severe reduction (SR) part of that pretreatment. Reoxidation ( $\text{O}_2$  100  $\mu\text{l}$  pulses, every 75 s) was performed at either 700 K (mild oxidation, MO) or 1273 K (severe oxidation, SO). Quantitative dynamic OSC measurements were performed by increasing the temperature in a stepwise manner and – during the isothermal steps (30 min) – alternately pulsing every 70 s  $\text{H}_2$  (100  $\mu\text{l}$ ) and  $\text{O}_2$  (100  $\mu\text{l}$ ) over the sample (15–20 mg, maintained in a flow of Ar of 25  $\text{ml min}^{-1}$ ). OSC was meas-

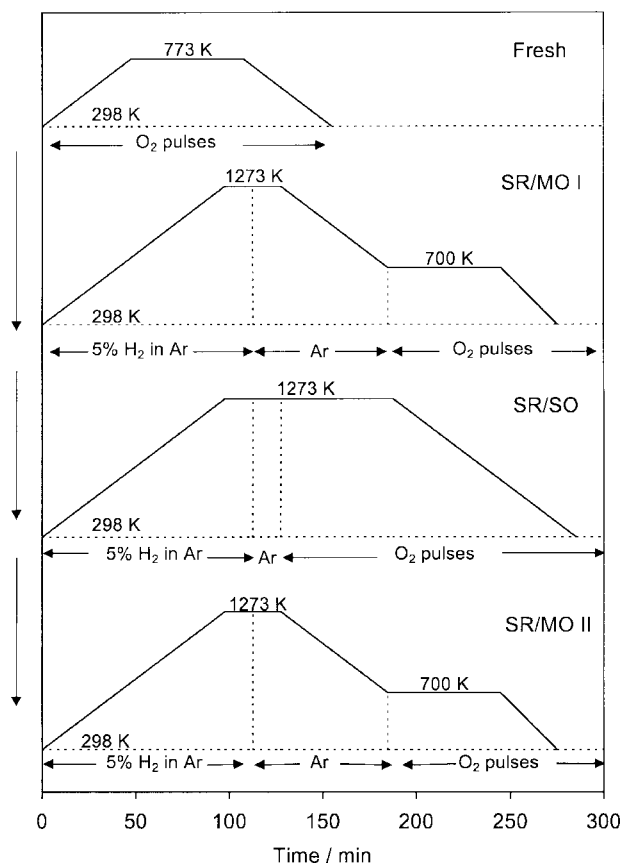


Figure 1. Cleaning/redox ageing procedures used. All ramping rates were  $10 \text{ K min}^{-1}$ . In reoxidation procedures the  $\text{O}_2$  pulses were made every 75 s using 100  $\mu\text{l}$  loops. All the treatments were performed consecutively on the same sample.

ured using a thermal conductivity detector as the uptake of  $\text{O}_2$  from the  $\text{O}_2$  pulse.

## 3. Results and discussion

### 3.1. TPR behaviour

Using the above-described ageing procedures, TPR profiles and the effects of redox ageing thereon are exemplified for both CZ-W and CZ-A sample in figure 2. Temperatures of maximum reduction rate and total OSC, as detected by pulsed reoxidation 700 K, are summarised in table 1.

Single peak profiles were obtained for both fresh samples (figure 2), consistent with the absence of significant phase inhomogeneity in the as-prepared samples [20]. Dramatic changes are induced by the redox ageing procedures. CZ-A shows an important improvement of the oxygen release property upon application of SR/MO I (figure 2(a), trace 2), the reduction peak being lowered to 537 K. To our knowledge, *this is the lowest reduction temperature ever reported for such type of materials*, which would suggest a high efficiency of such systems as OSC promoters. It should be noted that SR/MO I leads to a strong sintering of the surface area, which drops to  $4 \text{ m}^2 \text{ g}^{-1}$ , as detected by *in situ* BET measurement. The SR/SO treatment leads

to an increase in the temperature of reduction (figure 2(a), trace 3). This is substantially reversed by the second SR/MO sequence (figure 2(a), trace 4). These observations are consistent with previous reports.

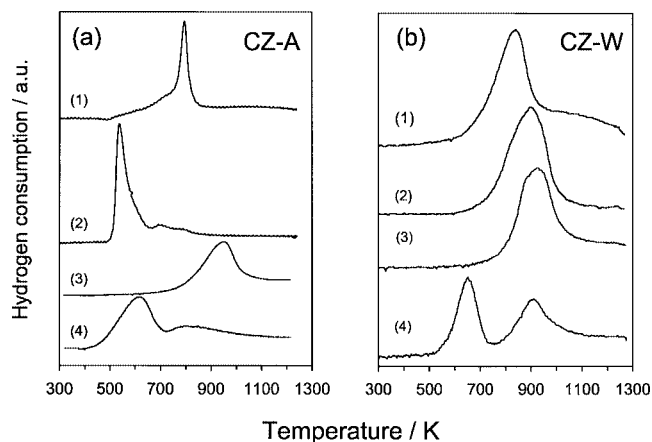


Figure 2. The effects of redox-aging on the TPR profiles of fresh  $\text{Ce}_{0.6}\text{Zr}_{0.4}\text{O}_2$  synthesised using (a) ethanol (CZ-A) or (b) water (CZ-W) as solvent: (1) fresh, (2) SR/MO I, (3) SR/SO and (4) SR/MO II. Compare figure 1 for pre-treatment details.

Table 1  
Summary of the TPR behaviour of CZ-W and CZ-A after various redox ageing procedures.

Sample	TPR <sup>a</sup>	$T_{\text{max}}$ (K)	$\text{O}_2$ uptake <sup>b</sup> ( $\text{ml g}^{-1}$ )	$\text{Ce}^{3+}$ (%)
CZ-W	1	840	18	75
	2	900	18	75
	3	930	18	75
	4	650, 900	18	75
CZ-A	1	795	19	80
	2	537	19	80
	3	950	17	71
	4	620, 800	17	71

<sup>a</sup> See figure 2.

<sup>b</sup> Measured by pulsing  $\text{O}_2$  at 700 K after the TPR experiment.

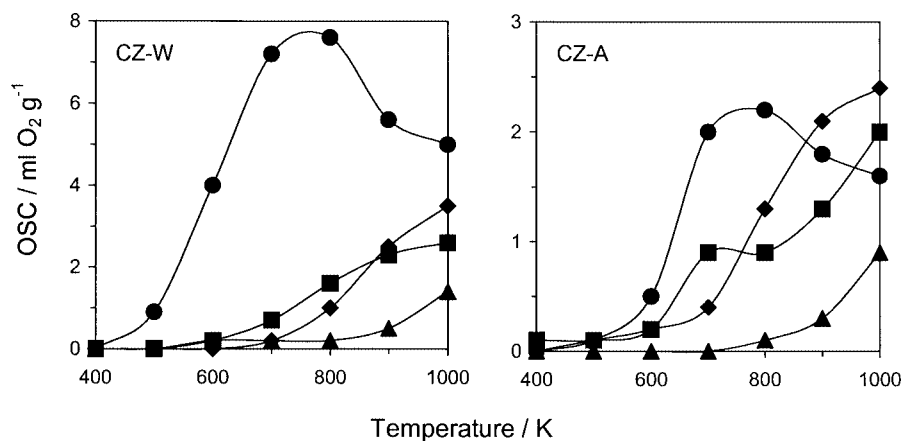


Figure 3. Dynamic OSC measured at the indicated temperature on  $\text{Ce}_{0.6}\text{Zr}_{0.4}\text{O}_2$ , synthesised using water (CZ-W) or ethanol (CZ-A) as solvent following the same treatments as in figure 2. The OSC values shown are the average of the last five pulses at each temperature and do not necessarily relate to a steady-state situation, which was not always reached (see text). (◆) Fresh, (▲) SR/SO, (■) SR/MO I and (●) SR/MO II.

The comparison with the TPR profiles of CZ-W is striking. In this case, no improvement of the reduction behaviour is observed upon application of SR/MO I (figure 2(b), trace 2). In fact, there is an upward shift to 900 K of the peak observed at 840 K in the fresh sample. No further modification of the TPR profile was observed upon application of at least three consecutive SR/MO sequences (data not reported). The SR/SO treatment results in a further slight upward shift of the TPR peak (figure 2(b), trace 3). However, as for CZ-A, SR/MO II results in an overall decrease in the reduction temperature (figure 2(b), trace 4), producing a significantly different profile from the others in the sequence. In summary, the most important point is that the ageing procedures induce very different TPR behaviour for these samples.

TPR behaviour of  $\text{CeO}_2\text{-ZrO}_2$  mixed oxides is strongly affected by a number of factors including synthesis conditions [21], phase composition [20], textural properties [11] and pre-treatment [16]. A rationale for the above-described TPR behaviour is behind the scope of this investigation; however, it can be commented that the low temperature reduction induced by the TPR/MO sequence is observed when either a non-homogeneous solid solution is used [22] or the sample was pre-sintered [23].

### 3.2. Dynamic OSC measurements

Figures 3 and 4 contain results of dynamic  $\text{H}_2$ -OSC investigations on these samples using  $\text{H}_2$  as reducing agent. With regard to the dynamic  $\text{H}_2$ -OSC results contained in figure 3, the values shown are the average of the last five pulses at each temperature and, for reasons outlined below, do not necessarily refer to a steady-state situation. However, mass balance considerations indicate that near-stoichiometric  $\text{H}_2 : \text{O}_2$  uptake was observed in these experiments. The aim of this study was to correlate the very favourable TPR behaviour of the SR/MO aged CZ-A sample with the ability to store/release oxygen under dynamic conditions.

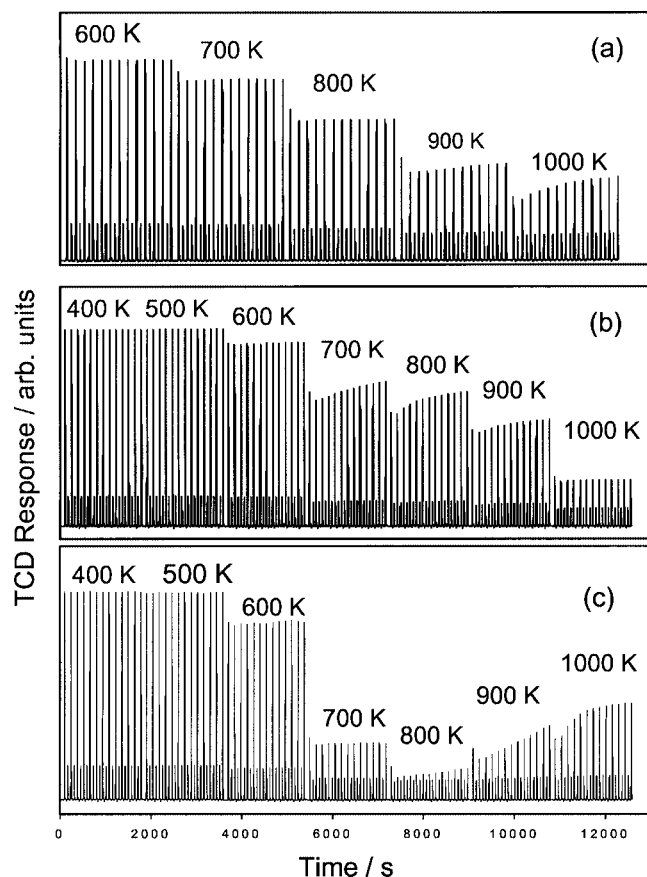


Figure 4. (a) Dynamic  $\text{H}_2$ -OSC pulse profiles measured at the indicated temperatures on  $\text{Ce}_{0.6}\text{Zr}_{0.4}\text{O}_2$ , synthesised using water (CZ-W) as solvent, after SR/MO I; (b) dynamic  $\text{H}_2$ -OSC pulse profiles measured at the indicated temperatures on  $\text{Ce}_{0.6}\text{Zr}_{0.4}\text{O}_2$ , synthesised using ethanol (CZ-A) as solvent, after SR/MO I; (c) dynamic  $\text{H}_2$ -OSC pulse profiles measured at the indicated temperatures on  $\text{Ce}_{0.6}\text{Zr}_{0.4}\text{O}_2$ , synthesised using ethanol (CZ-A) as solvent, after SR/MO II. Notice that  $\text{O}_2$  and  $\text{H}_2$  are alternately pulsed during the experiment.

For the fresh samples, appreciable OSC values are measured starting from about 800 K. This is fairly consistent with the fresh TPR profiles of the samples, which feature reduction peak maxima, respectively, at 795 and 840 K. At 1000 K, which is the maximum temperature here investigated, a dynamic OSC of  $3.5 \text{ ml-O}_2 \text{ g}^{-1}$  is observed over fresh CZ-W (figure 3(a)). In contrast, dynamic OSC of CZ-A is about 30% lower, despite the fact that comparable total OSC were measured on the two samples (table 1).

Comparison of figure 3 with figure 2 reveals that the changes induced in the TPR profiles by the series of treatments are not directly reflected in dynamic  $\text{H}_2$ -OSC investigations. Certain general trends are followed. Thus, SR/SO lowers the dynamic OSC values measured, while SR/MO II causes them to increase again. In particular, the improvement in the TPR profile of CZ-W after SR/MO II (figure 2(b), trace 4) is clearly apparent: significant  $\text{O}_2$  and  $\text{H}_2$  uptakes were measured at 600 K. This is a rather low temperature if the low surface area of the sample is considered. Generally speaking, dynamic OSC measurements on  $\text{CeO}_2$ - $\text{ZrO}_2$  mixed oxides of comparable surface area were

reported at and above 673 K, which typically represents the onset temperature for the dynamic OSC when CO is employed as reducing agent [24], even though CO-TPR experiments carried out on high surface area mixed oxides showed that reduction can start at temperatures as low as 473 K [25]. More important perhaps than the temperature of on-set of dynamic  $\text{H}_2$ -OSC however are the values measured at higher temperature, truly remarkable for dynamic measurements.

However, other observations suggest that the two techniques do not show a direct correspondence. For example, the value obtained for the dynamic  $\text{H}_2$ -OSC of the CZ-A sample after SR/MO I is significantly lower than would be expected on the basis of the corresponding TPR profile. In addition, after SR/MO II, both samples show significant decreases in dynamic OSC values at the highest temperatures of investigation; as well as an inversion of the values measured for the fresh and SR/MO I treated samples as the temperature increases. An explanation of these observations may be found in the pulse profiles observed in the experiments. Figure 4 (a) and (b) reports typical experiments carried out on CZ-A and CZ-W after SR/MO I. There are clear indications of a transient behaviour as the temperature of the dynamic  $\text{H}_2$ -OSC measurement is progressively increased: the dynamic OSC of the CZ-A observed at 700 K appears to decrease gradually with time part (b), indicating that an *in situ* modification of the active species is occurring. This deactivation is even more apparent at 800 and 900 K. This behaviour is also observed in the case of the CZ-W sample (part (a)), but only becomes significant at 900 and 1000 K. This deactivation phenomenon was observed in all such dynamic experiments, and was always evident at lower temperatures for the CZ-A sample, which appears to be very unstable after treatments which induce very low-temperature TPR profiles. This suggests a lower "thermal stability" of the dynamic OSC property in this sample. The most remarkable instance of the phenomenon is illustrated in figure 4, part (c), which shows the dynamic pulse sequence obtained after SR/MO II. It should also be noted that, while reproducible for each ageing procedure, the severity of the effect differed greatly across the series, the fresh profiles being least affected.

For the purposes of comparison, dynamic OSC measurements were also made using CO as the reducing agent (figure 5). These were performed immediately following dynamic  $\text{H}_2$ -OSC investigations. Accordingly, due to the above-mentioned *in situ* deactivation, steady-state values were measured. It appears that CO is a more effective reducing agent than  $\text{H}_2$  for these sample. For the fresh and SR/MO treated samples, full uptake of CO but not  $\text{H}_2$  was observed at 1000 K under identical conditions of investigation. The detrimental effect of SR/SO upon reductions, as suggested by the TPR profiles, is also apparent in that full uptake of CO was not observed up to 1000 K after this treatment. A set of data was also obtained following the SR/MO treatment, without an intermediate experiment involving  $\text{H}_2$  and  $\text{O}_2$  pulses. As with analogous experiments involving  $\text{H}_2$ , the pulse profiles in these experiments were unsteady,

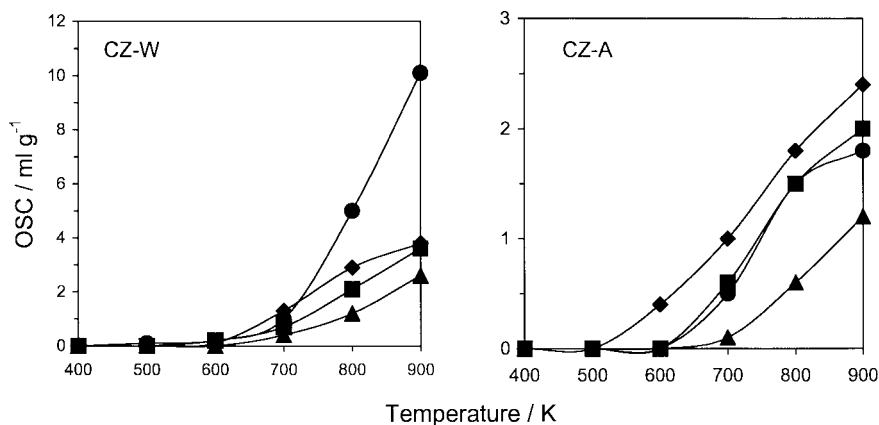


Figure 5. Dynamic CO-OSC measured at the indicated temperature on  $\text{Ce}_{0.6}\text{Zr}_{0.4}\text{O}_2$ , synthesised using water (CZ-W) or ethanol (CZ-A) as solvent. (♦) Fresh, (▲) SR/SO, (■) SR/MO I and (●) SR/MO II.

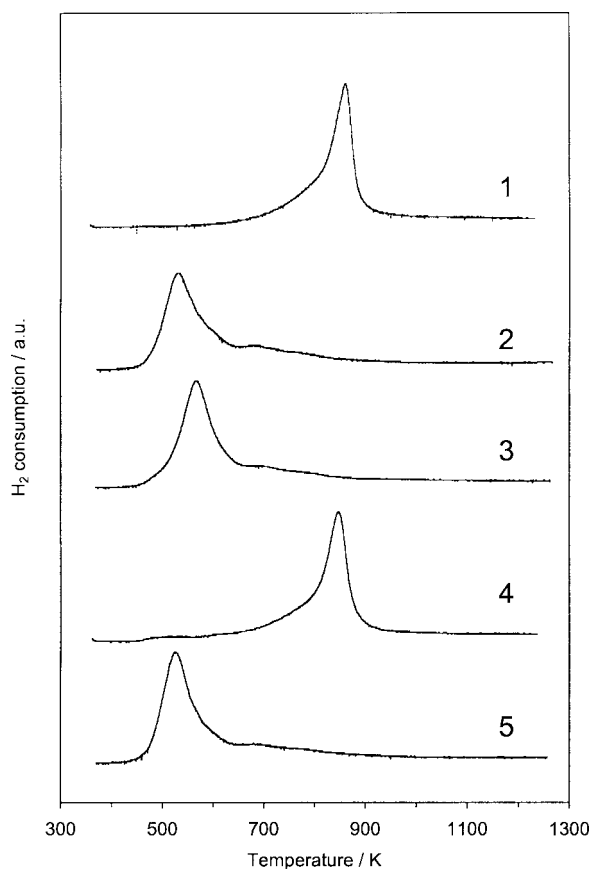


Figure 6. TPR profiles of CZ-A: (1) fresh, (2) after SR/MO followed by dynamic  $\text{H}_2$ -OSC and pulsed oxidation at 500 K, (3) after SR/MO followed by dynamic  $\text{H}_2$ -OSC and pulsed oxidation at 600 K, (4) after SR/MO followed by dynamic  $\text{H}_2$ -OSC experiment from 400 to 1000 K, (5) after SR/MO followed by heating in He for 2 h and pulsed oxidation at 700 K.

beginning at 700 K, and remarkably so at 800 K. However, it should be noted that the manifestation of the effect was different for the two reducing agents. CZ-W after SR/SO I appears to be the most effective system. Good mass balance was observed in all of these experiments.

To obtain some insight into this deactivation phenomenon, a separate sequence of experiment was conducted us-

ing the CZ-A sample, in which TPR profiles were obtained (during SR/MO) after dynamic  $\text{H}_2$ -OSC investigations had been conducted at various temperatures. These dynamic measurements were followed by  $\text{O}_2$  pulses at the same temperature to ensure oxidation of the sample. The aim was to determine the effect of the dynamic experiments on TPR behaviour. The TPR profiles thus recorded are reported in figure 6. The profile observed after the dynamic OSC measured at 500 K is comparable with that reported in figure 2(a), trace 2, indicating that species of equivalent reduction behaviour were obtained in the two experiments. However, when the TPR is performed after the dynamic OSC experiment at 600 K, the reduction peak is shifted to a higher temperature, indicating that modifications of the reduction behaviour had occurred in the dynamic OSC experiment. Consistently, after the dynamic OSC carried out at 1000 K a full displacement of the reduction peak to a temperature comparable to that of the fresh CZ-A (figure 2(a), trace 1) was observed. No shift of the reduction peak to higher temperature was observed in the TPR profile obtained after subjecting the sample to a thermal treatment (2 h, He) at 700 K, followed by  $\text{O}_2$  pulses at 700 K.

The extent of the changes induced by dynamic measurements show a dependence on the treatment. Thus, before the SR/SO treatment, dynamic  $\text{H}_2$ -OSC measurements to 1000 K are sufficient to fully reverse the TPR profile. After the SR/SO treatment, dynamic measurements do not affect the profile. Once a further SR/MO treatment has been performed, the changes induced in the TPR profile by the dynamic measurements are intermediate. A further SR treatment is necessary to produce a TPR identical to that in figure 2(a), trace 4.

#### 4. Conclusions

Investigation of the redox properties of two  $\text{Ce}_{0.6}\text{Zr}_{0.4}\text{O}_2$  materials prepared via a citrate route showed that materials which release oxygen at very mild temperature under TPR conditions can be made by appropriately pre-treating the sample. When ethanol is employed as a solvent reduc-

tion at a temperature as low as 537 K could be achieved after a TPR/mild oxidation treatment. However, due to the fact that these materials show a high sensitivity to oxidative treatments, the improved reduction behaviour is of a transitory nature, *in situ* deactivation of dynamic OSC being observed even at relatively low temperatures. An important result of this investigation is that we have obtained a straightforward indication that a  $CeO_2$ – $ZrO_2$  material which shows a very favourable TPR profile with low-temperature reduction may be rather ineffective as an OSC material. Under driving conditions high-temperature oxidative conditions are easily met, while prolonged rich type of excursions of the air-to-fuel ratio are infrequent. This indicates TPR analysis may not be appropriate for the investigation of the OSC property and that caution should be exercised before the superior performances of a  $CeO_2$ – $ZrO_2$  material can be inferred from an analysis of the TPR behaviour only.

### Acknowledgement

University of Trieste, CNR (Roma) Programmi Finalizzati “Materiali Speciali per Tecnologie Avanzate II”, Contract no. 97.00896.34 and “Regione Friuli Venezia-Giulia, Fondo regionale per la ricerca”, are gratefully acknowledged for financial support.

### References

- [1] J. Kaspar, P. Fornasiero and M. Graziani, *Catal. Today* 50 (1999) 285, and references therein.
- [2] A. Laachir, V. Perrichon, A. Badri, J. Lamotte, E. Catherine, J.C. Lavalley, J. El Fallah, L. Hilaire, F. Le Normand, E. Quemere, N.S. Sauvion and O. Touret, *J. Chem. Soc. Faraday Trans.* 87 (1991) 1601.
- [3] A. Trovarelli, *Catal. Rev. Sci. Eng.* 38 (1996) 439.
- [4] H.C. Yao and Y.F. Yu Yao, *J. Catal.* 86 (1984) 254.
- [5] K.C. Taylor, *Catalysis – Science and Technology*, eds. J.R. Anderson and M. Boudart (Springer, Berlin, 1984) ch. 2, pp. 119–170.
- [6] A. Jones and B. McNicol, *Temperature-Programmed Reduction for Solid Materials Characterization* (Dekker, New York, 1986).
- [7] F.M.Z. Zotin, L. Tournayan, J. Varloud, V. Perrichon and R. Frety, *Appl. Catal. A* 98 (1993) 99.
- [8] J. Kaspar, M. Graziani and P. Fornasiero, *Handbook on the Physics and Chemistry of Rare Earths: The Role of Rare Earths in Catalysis*, eds. K.A. Gschneidner, Jr. and L. Eyring (Elsevier, Amsterdam, 2000) ch. 184, pp. 159–267.
- [9] C. Norman, MEL Chemicals, Manchester (UK) (2000), personal communication.
- [10] G. Balducci, P. Fornasiero, R. Di Monte, J. Kaspar, S. Meriani and M. Graziani, *Catal. Lett.* 33 (1995) 193.
- [11] P. Fornasiero, G. Balducci, R. Di Monte, J. Kaspar, V. Sergo, G. Gubitosa, A. Ferrero and M. Graziani, *J. Catal.* 164 (1996) 173.
- [12] P. Fornasiero, R. Di Monte, G. Ranga Rao, J. Kaspar, S. Meriani, A. Trovarelli and M. Graziani, *J. Catal.* 151 (1995) 168.
- [13] N. Izu, T. Omata and S. Otsuka-Yao-Matsuo, *J. Alloys Compd.* 270 (1998) 107.
- [14] S. Otsuka-Yao-Matsuo, T. Omata, N. Izu and H. Kishimoto, *J. Solid State Chem.* 138 (1998) 47.
- [15] S. Otsuka-Yao, H. Morikawa, N. Izu and K. Okuda, *J. Jpn. Inst. Metals* 59 (1996) 1237.
- [16] R.T. Baker, S. Bernal, G. Blanco, A.M. Cordon, J.M. Pintado, J.M. Rodriguez-Izquierdo, F. Fally and V. Perrichon, *J. Chem. Soc. Chem. Commun.* (1999) 149.
- [17] T. Masui, T. Ozaki, K. Machida and G. Adachi, *J. Alloys Compd.* 292 (1999) L8.
- [18] M. Yashima, H. Arashi, M. Kakihana and M. Yoshimura, *J. Am. Ceram. Soc.* 77 (1994) 1067.
- [19] M. Daturi, C. Binet, J.C. Lavalley, H. Vidal, J. Kaspar, M. Graziani and G. Blanchard, *J. Chim. Phys.* 95 (1998) 2048.
- [20] P. Vidmar, P. Fornasiero, J. Kaspar, G. Gubitosa and M. Graziani, *J. Catal.* 171 (1997) 160.
- [21] S. Rossignol, Y. Madier and D. Duprez, *Catal. Today* 50 (1999) 261.
- [22] T. Egami, W. Dmowski and R. Brezny, SAE 970461 (1997).
- [23] P. Fornasiero, J. Kaspar and M. Graziani, *Appl. Catal. B* 22 (1999) L11.
- [24] A. Trovarelli, F. Zamar, J. Llorca, C. de Leitenburg, G. Dolcetti and J.T. Kiss, *J. Catal.* 169 (1997) 490.
- [25] Y. Madier, C. Descorme, A.M. LeGovic and D. Duprez, *J. Phys. Chem. B* 103 (1999) 10999.